Supporting Information for

Multifunctional AIEgen-based luminescent metal–organic frameworks with coordination-induced emission for chemical sensing

Wei Wei[a#], Yaru Zhang[a#], and Xue-Bo Yin[*,a,b] Yan Xia[*,a]

[a]Research Center for Analytical Science and Tianjin Key Laboratory of Biosensing and Molecular Recognition, College of Chemistry, Nankai University, Tianjin, 300071, China.

[b]College of Chemistry and Chemical Engineering, Shanghai University of Engineering Science, Shanghai, 201620, China

#Wei wei and Yaru zhang contributed equally to this work.

[*]Xue-Bo Yin, E-mail: xbyin@nankai.edu.cn

[*]Yan Xia, E-mail: nkxiayan@nankai.edu.cn

Table of Content

1. Reagents

Vitamin B1, methyl 4-formylbenzoate, 2, 5-dimethyl pyrazine, ammonium acetate and europium(III) nitrate hexahydrate ($Eu(NO_3)_3·6H_2O$) were purchased from Aladin Ltd. (Shanghai, China). $Zn(NO_3)_2$, $AgNO_3$, $CaCl_2$, $NiSO_4·6H_2O$, $CoCl_2·6H_2O$, $Fe(NO_3)_3·9H_2O$, $FeSO_4$, $MgSO_4$, $MnCl_2$, $Pb(NO_3)_2$, KSCN, $NaHCO_3$, $CuSO_4·5H_2O$ and Na_2SO_4 were obtained from Guangfu technology development Co., Ltd. (Tianjin, China). Ammonium acetate was obtained from Macklin Bionchemistry Co., Ltd., Shanghai, China. N, N'-dimethylformamide, acetic anhydride, diethyl ether, ice acetic acid, N, N'-dimethylacetamide, concentrated hydrochloric acid and tetrahydrofuran were purchased from Concord Chemical Research Institute (Tianjin, China). KIO_3, HNO_3, CH_3COONa, $KBrO_3$, $KMnO_4$, KNO_3, NaOH, $NaBH_4$, $AlCl_3$, $CrCl_3$, NaCl, K_2CrO_7, KBr, $MnCl_2$, KI were provided by Fengchuan Chemical Reagents (Tianjin, China). glycine, alanine, leucine, valine, cyseins, tyrosine, histidine, lysine, arginine were obtained from Sigma-Aldrich (Shanghai, China). All the chemicals were obtained at least of analytical grade and used without further purification. The ultrapure water used throughout all the experiments was purified through Water Purifier Nanopure water system (18.3 MΩ cm).

2. Instrumentations

Scanning Electron Microscopy (SEM) images were recorded with JSM-7500F, Japan. Transmission electron microscopy (TEM) images and EDX studies were carried out with the TecnaiG2 F20, FEI Co. (America) operated at an accelerating voltage of 200 kV. Most of the steady-state fluorescence experiments were carried out on a FL-4600 Fluorescence Spectrometer, Hitachi, Japan, equipped with a plotter unit and a quartz cell (1 cm × 1 cm). The measurement of Cu and Fe element after Cu-MOF detection carried out on a Spectro Blue inductively coupled plasma-optical emission spectroscopy (ICP-OES) (Spectro, Germany). N_2 adsorption-desorption and CO_2 adsorption-desorption isotherm weere recorded with ASAP2020/Tristar 3000 surface area and pore analyzer at 274 K. NMR experiments were performed on AV 400, Bruker, America.

Elemental analysis was carried out on a vario EL CUBE analyzer (Elementary, Germany). Thermogravimetric analysis (TGA) was performed on a PTC-10ATG-DTA analyzer heated from 20 °C at a ramp rate of 15 °C min^{-1} under air. PXRD patterns from an angle range of 10° to 60° were recorded on a D/max-2500 diffractometer (Rigaku, Japan) using Cu Kα radiation (λ = 1.5418 Å) with a scanning speed of 8° min^{-1} and a step size of 0.02° in 2θ. Fourier transform infrared spectroscopy (FT-IR) was obtained by Nicolet iS50 Fourier transform infrared spectroscopy, over the ranging from 400 to 4000 cm^{-1}. The UV−vis absorption spectra were obtained on the U-3600 visible spectrophotometer (Shimadzu, Japan). The images are taken by mobile phone.

3. Synthesis and method

3.1 Synthesis of 2,3,5,6-tetrakis(4-carboxyphenyl)pyrazine (TCPP)

Synthesis of dimethyl-4,4'-(2-hydroxyacetyl)dibenzoate, 1a

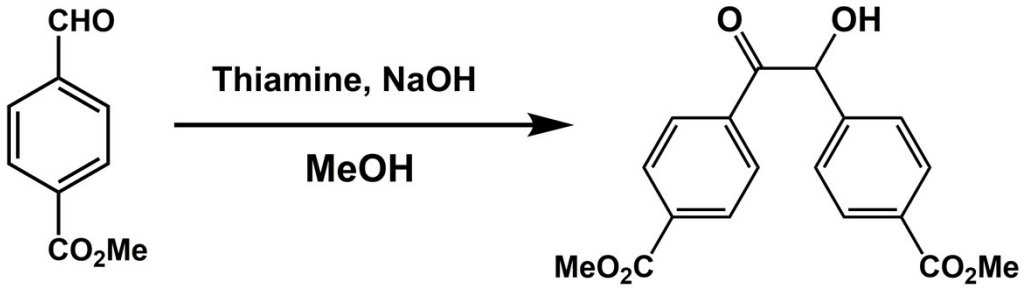

Compound 1a was synthesized according to the published method with minor modifications.[1] Vitamin B1 (720 mg, 2.13 mmol) was added to the mixture of methanol (15 ml) and water (5 ml) under ice bath. Then, sodium hydroxide solution (2 mL, 2 M) was added in the above solution drop-wise to adjust the pH to 9−10. Under rigid stir, methyl 4-formylbenzoate (6.0 g, 36.55 mmol) was added into the above solution. After being stirred 1 h in the ice water bath, the reaction mixture was heated at 60 °C for 1 h and at 85 °C for 1 h. After cooling and filtering, the product compoud 1a was obtained followed with washed by water, methanol and diethyl ether,respectively, drying at 60 °C.

^{1}H NMR (400MHz, $CDCl_3$) δ(ppm): 8.14 (d, J=7.6Hz, 2H), 8.02 (d, J=7.6 Hz, 2H), 7.92(d, J= 8.8

Hz), 7.57(d, J=8.8Hz, 2H), 6.50(d, J=6.6Hz), 6.18(d, J=7.2 Hz), 3.56 (s, 3H).

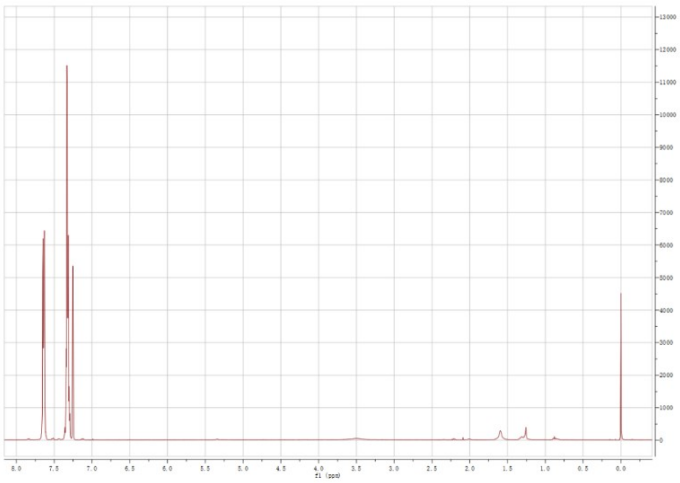

Figure S1. ^{1}H NMR spectrum of dimethyl-4,4'-(2-hydroxyacetyl)dibenzoate.

Synthesis of 2,3,5,6-tetrakis(4-methoxycarbonyl)phenyl)pyrazine, 1b

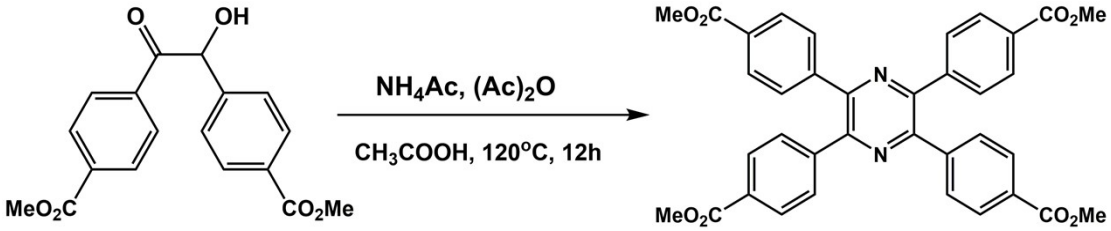

1b was synthesised by following the literature procedure[2]. Acetic anhydride (765 mg, 7.50 mmol) was added into the mixture of compound 1a (1.64 g, 5.00 mmol) and ammonium acetate (1.155 g, 15.00 mmol) in 5 mL of acetic acid. After being stirred for 12 h at 120 °C under N_2, the precipitate was formed.Filtration and washing with H_2O and diethyl ether afforded 2,3,5,6tetrakis(4-(methoxycarbonyl)phenyl)pyrazine as a yellow solid

^{1}H NMR (400 MHz, DMSO-d6): δ = 8.05 (dt, J1 = 9.0 Hz, J2 = 2.1 Hz, 8H), 8.45 (dt, J1 = 8.7 Hz, J2 = 1.8 Hz, 8H), 3.95 (s, 12H). ^{13}C NMR (100 MHz, DMSO-d6): δ = 166.6, 148.2, 142.0, 130.6, 129.9, 129.7, 52.5.

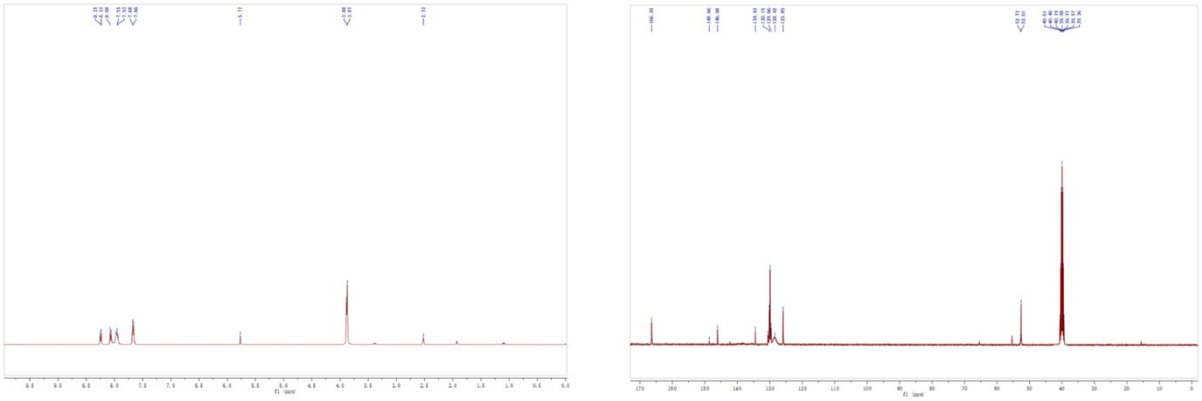

Figure S2. ^{1}H NMR and ^{13}C NMR spectrum of 2,3,5,6-tetrakis(4-methoxycarbonyl)phenyl) pyrazine.

Synthesis of 2,3,5,6-tetrakis(4-carboxyphenyl)pyrazine (H_4TCPP)

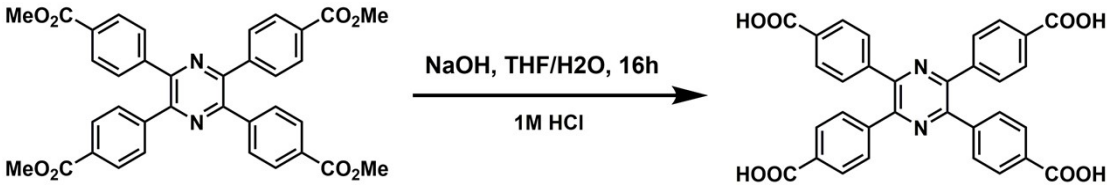

To a solution of 2,3,5,6-tetrakis(4-(methoxycarbonyl)phenyl)pyrazine (1.021 g, 1.66 mmol) in THF-H_2O (1:1, 30 mL) was added NaOH (0.796 g, 19.90 mmol). The mixture was refluxed for about 12 h and THF was evaporated. The solution was acidified to pH of 4−5 with HCl (2 M). The precipitate was filtered and washed with H_2O to obtain H_4TCPP as a yellow solid.

^{1}H NMR (400 MHz, DMSO-d6): δ = 12.76 (br, 4H), 7.94 (d, J = 8.8 Hz, 8H), 7.59 (d, J = 8.8 Hz, 8H). 13C NMR (100 MHz, DMSO-d6): δ = 167.1, 146.1, 141.4, 134.1, 128.8, 129.3.

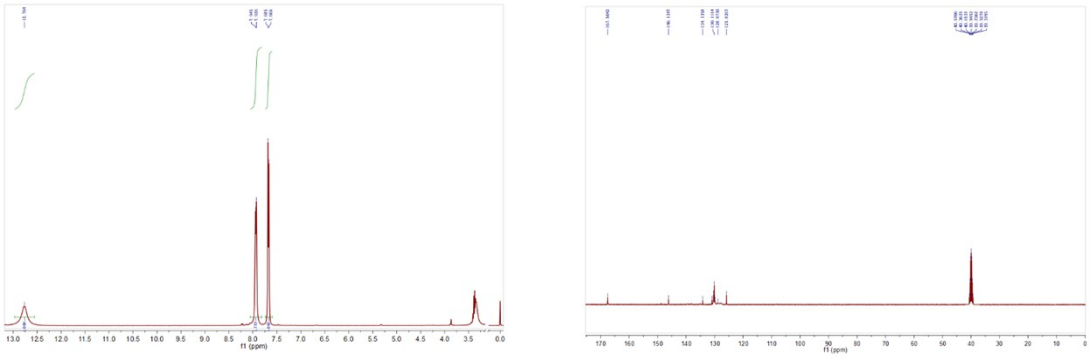

3.2 Synthesis of AMOFs

Figure S3. ^{1}H NMR and ^{13}C NMR spectrum of 2, 3, 5, 6-tetrakis (4-carboxyphenyl)pyrazine.

3.2.1 Synthesis of Cu-MOF.

$Cu(COOCH_3)_2 \cdot 2H_2O$ (7.98 mg, 0.04 mmol) and TCPP(6.0 mg, 0.01 mmol) were dissolved in the mixture of N, N'-dimethylacetamide (DMF 1.0 mL), ethanol (0.5 mL) and pure water (0.5 mL), and then HNO_3 (100 μL) was added[3]. The as-obtained mixture was transferred to a stainless steel Teflon-lined autoclave of 20 mL capacity. After being sonicated for 10 min, the mixture was maintained at 120 °C for 30 h under static conditions. After naturally cooling to room temperature, the product was washed with DMF and ethanol. Finally, the samples were dried under 50 °C. The preparation methods of Cu-MOF with different morphology were illustrated in Table S1.

3.2.2 Synthesis of M-MOFs.

The synthesis of M-MOF (M=Fe^{3+}, Eu^{3+}) was similar to that of Cu-MOF, only replace $Cu(COOCH_3)_2 \cdot 2H_2O$ with $Fe(NO_3)_3 \cdot 9H_2O$(13.57mg,0.04mmol), $Eu(NO_3)_3 \cdot 6H_2O$ (17.84 mg, 0.04 mmol), respectively.

3.3 Experiment for the Luminescent Properties of AMOFs.

AMOFs were well-dispersed in DMF with ultrasound for about 10 min, and then different amounts of water were added into DMF to detect the AIE effect of AMOFs. In addition, the same amounts of AMOFs was dissolved in different solvent to detect the fluorescence of AMOFs in the different organic solvent.

3.4 Experiment for the Detection of target.

0.5 mg of Cu-MOF was well-dispersed in a solution of 50 mL of DMF with stirring for about 10 min, and then diverse amounts of iron ions were added to a quartz cuvette containing 2 mL of DMF suspension of Cu-MOF (0.01 $mg \cdot mL^{-1}$) for the luminescent detection experiment. The experiment for the detection of Arginine is same as that of the detection of iron ions.

3.5 Limit of detection

According to the International Union of Pure and Applied Chemistry (IUPAC), the detection limit is calculated with followed formula[6].

$$LOD=kS_b/a$$

Where LOD is limit of detection, k=3 for spectral chemical analysis, and a is the sensitivity of a sensor (i.e. the slope of the calibration curve). The confidence level corresponding to k = 3 is about 90%. S_b is the standard deviation of the blank signal.

4. Figures and Tables

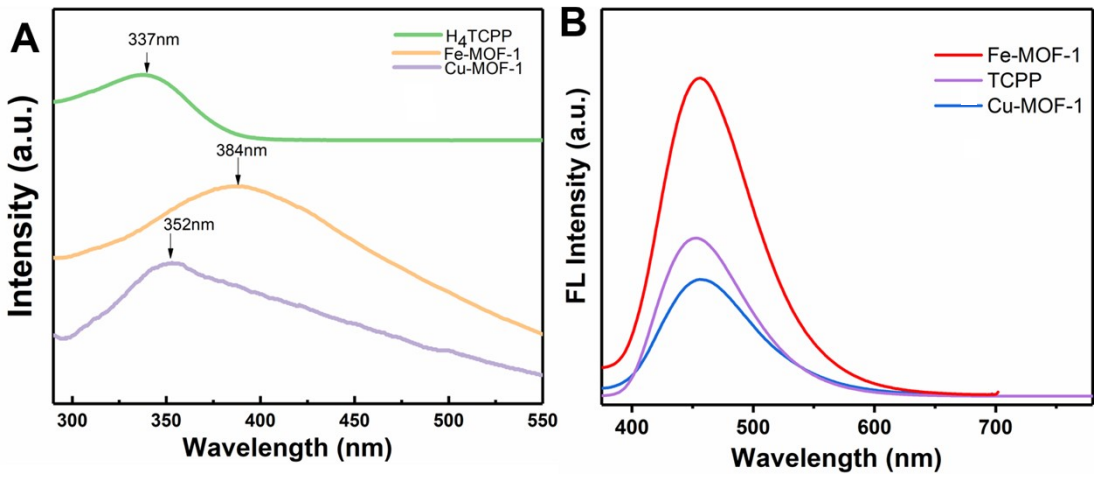

Figure S4. (A) UV-Visible absorption spectra of TCPP, Fe-MOF, and Cu-MOF. (B) Fluorescence profiles of TCPP, Fe-MOF, and Cu-MOF.

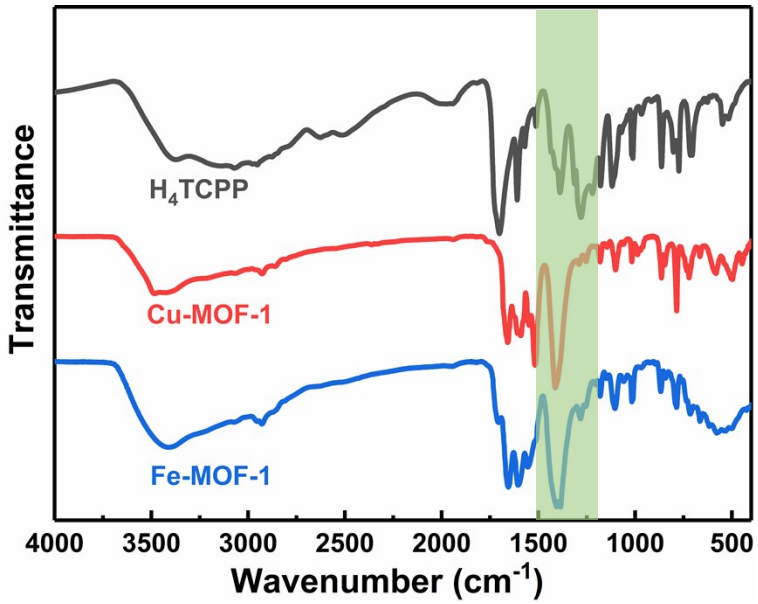

Figure S5. Fourier transform infrared spectra of TCPP, Cu-MOF and Fe-MOF.

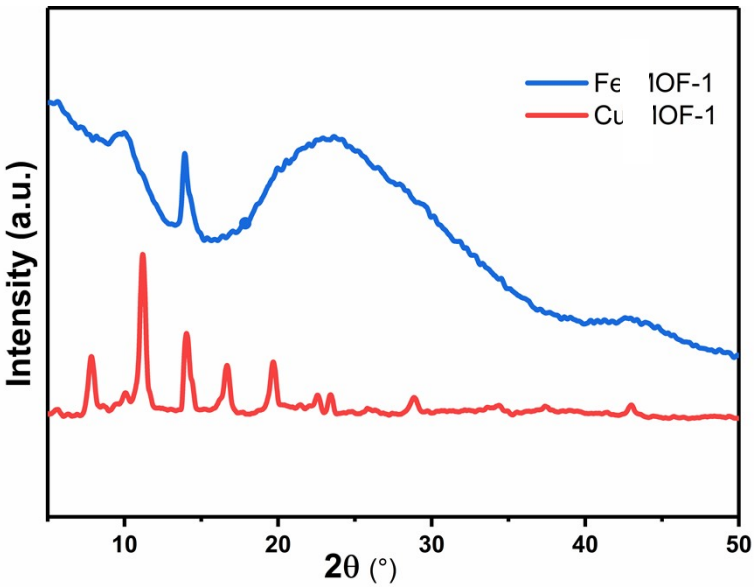

Figrue S6. The PXRD pattern of Fe-MOF and Cu-MOF.

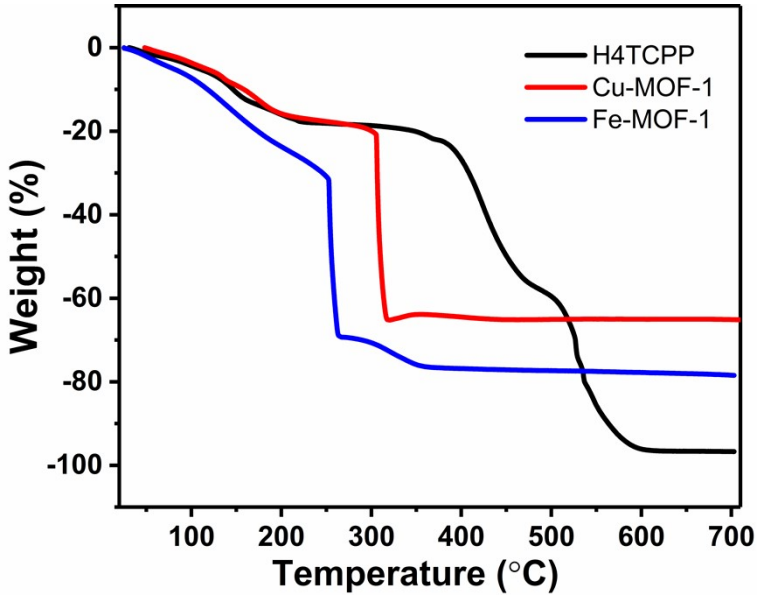

Figure S7. Thermogravimetric analysis of TCPP, Cu-MOF and Fe-MOF.

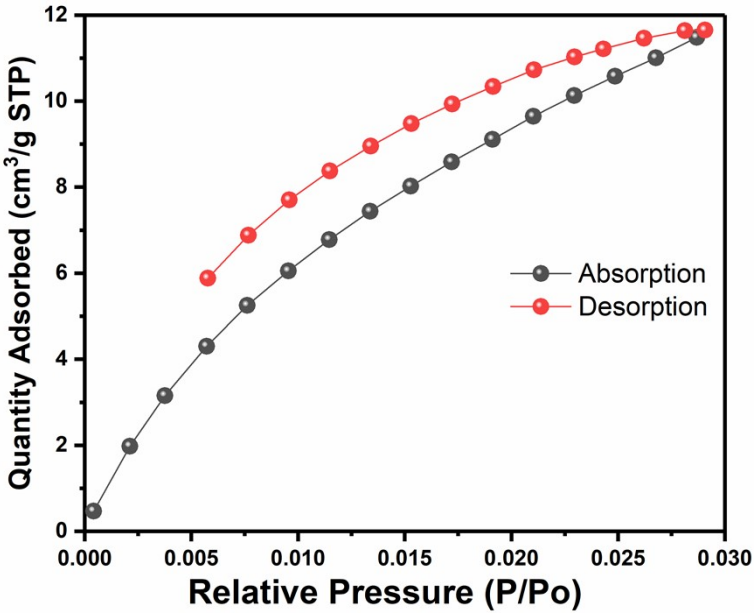

Figure S8. CO_2 adsorption and desorption isotherm of Cu-MOF.

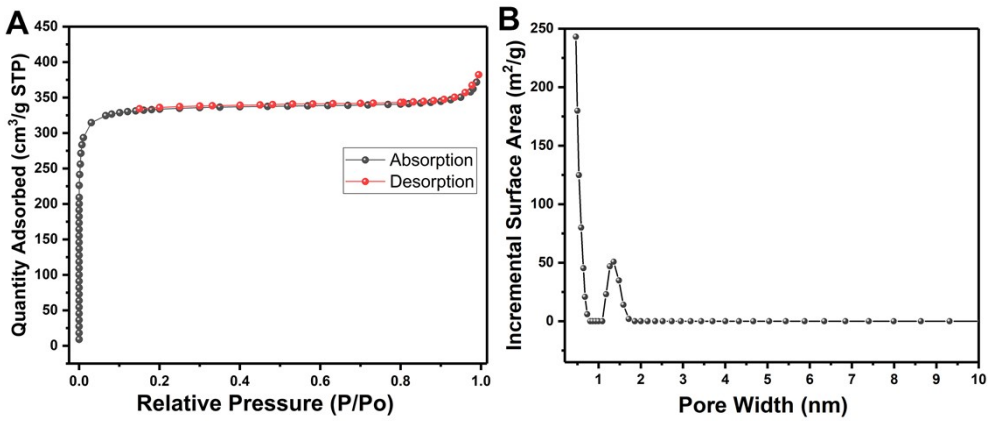

Figure S9. (A) Nitrogen adsorption and desorption isotherm of Cu-MOF. (B) The corresponding pore size distribution calculated from N_2 adsorption isotherms.

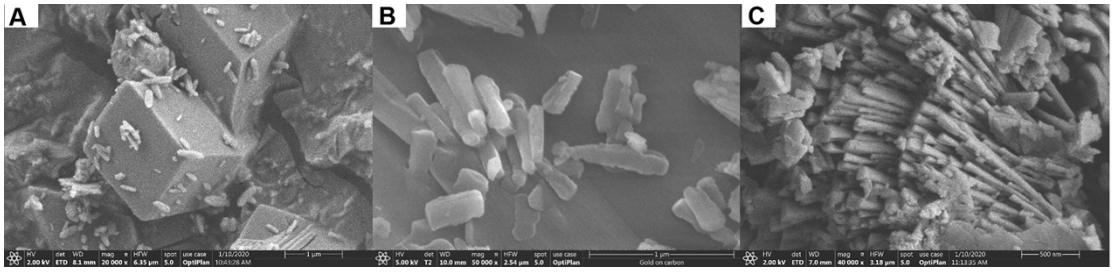

Figure S10. Scanning electron microscopy(SEM) images of Cu-MOF with different synthesized temperature: (A) 85℃,(B) 120℃ (C) 150℃(Scale bar: A,B: 1 μm and C:500 nm).

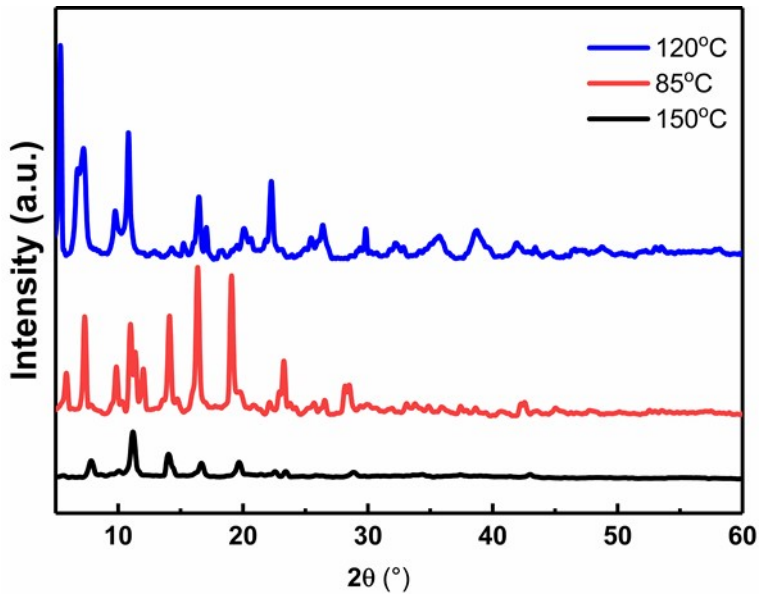

Figure S11. The PXRD pattern of Cu-MOF with different synthesis temperature.

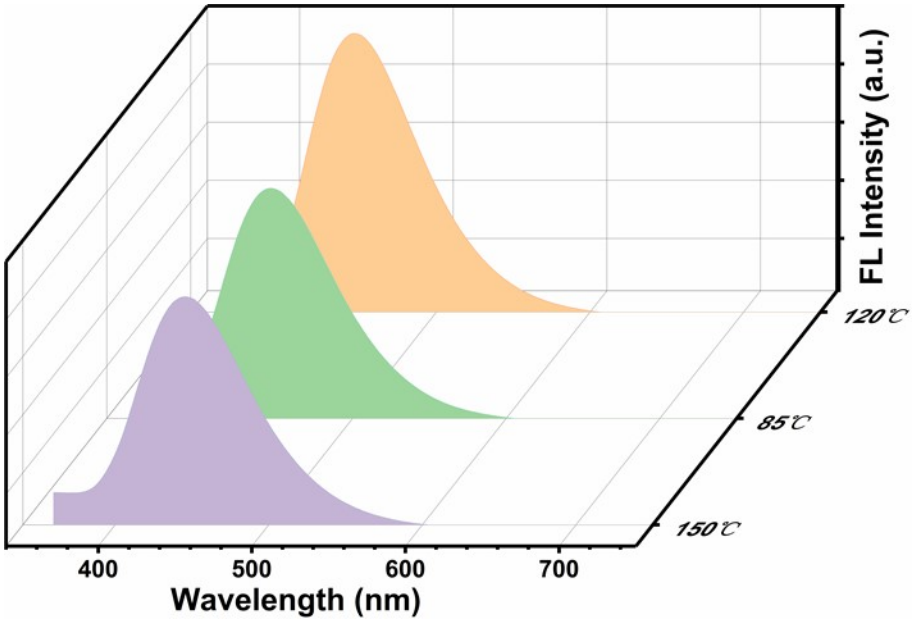

Figure S12. The fluorescence emission spectra of Cu-MOF with different synthesis temperature.

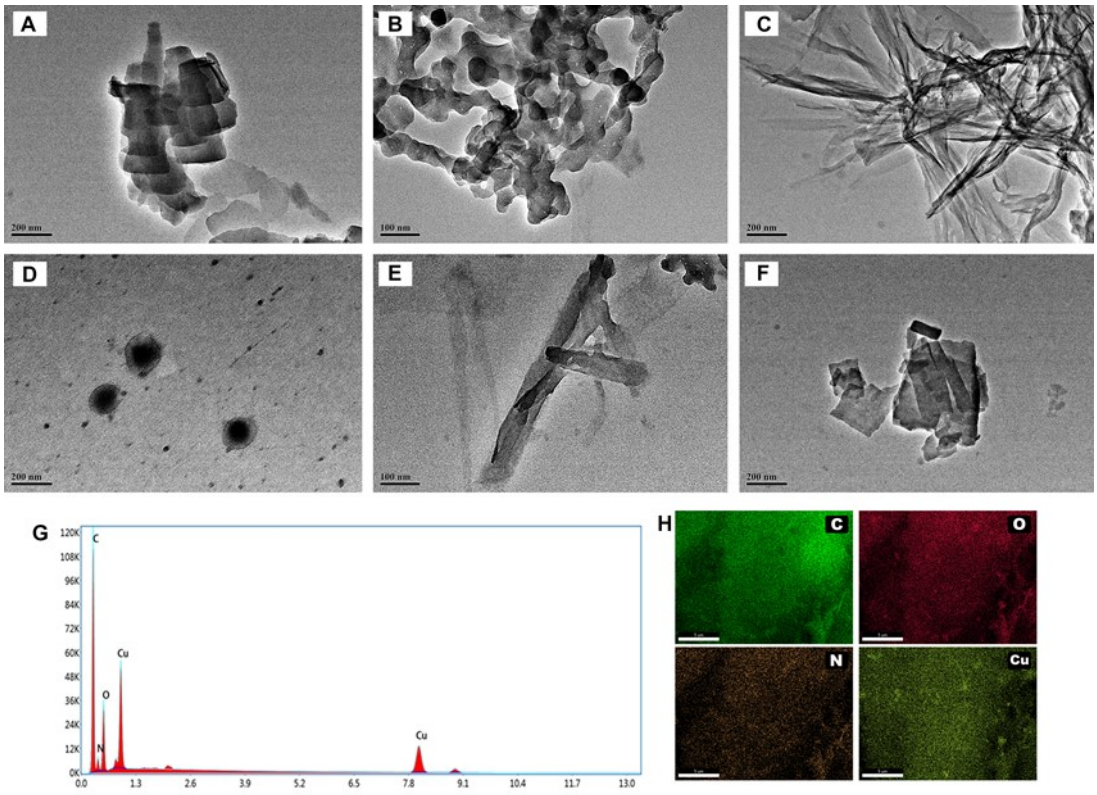

Figure S13. High-resolution transmission electron microscopy (HRTEM) images of Cu-MOF with different morphologies: (A) sphere, (B) nanosphere, (C) bulk, (D) rod, (E) nanorod, and (F) nanosheet. (Scale bar: A, C, D and F: 200 nm; B and E: 100 nm). (G) EDX spectrum of bulk Cu-MOF composite coating. (E) EDX elemental mapping images of C, N, O and Cu for Cu-MOF.

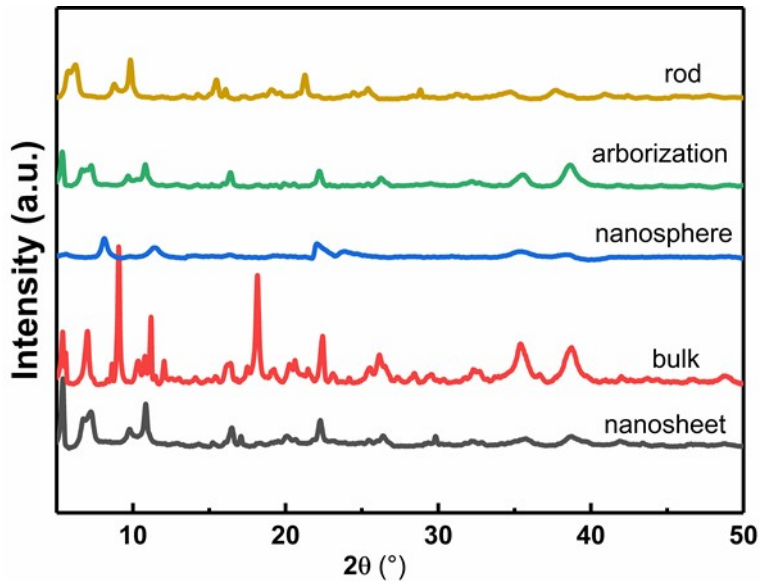

Figure S14. PXRD patterns of different morphology Cu-MOF.

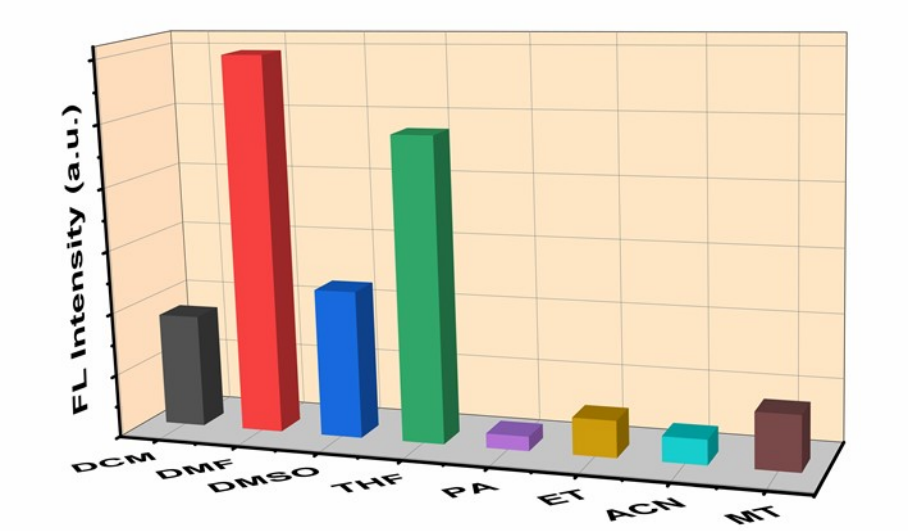

Figure S15. Flourescence emission spectra of Cu-MOF in different solvent (DCM: Dichloromethane, DMF: N,N-Dimethylformamide, DMSO: Dimethyl sulfoxide, THF: Tetrahydrofuran, PA: Propanone, ET: Ethanol, ACN: Acetonitrile, MT: Methanol).

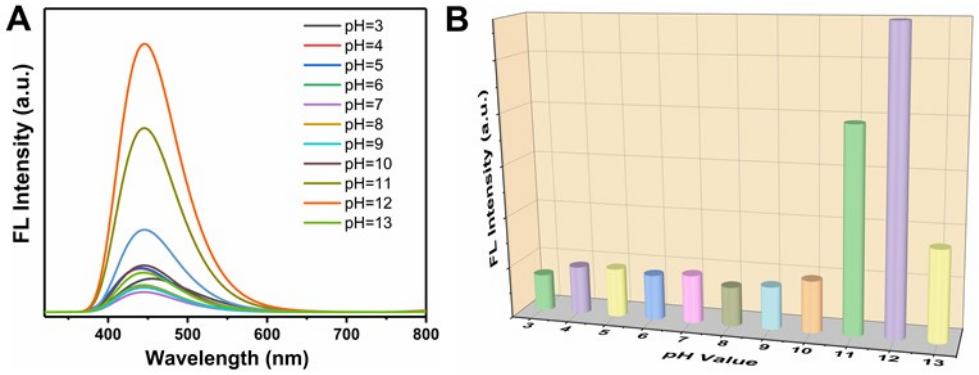

Figure S16. (A)FL spectra of Cu-MOF in different pH solution. (B) The effect of pH on the fluorescence intensity of the Cu-MOF.

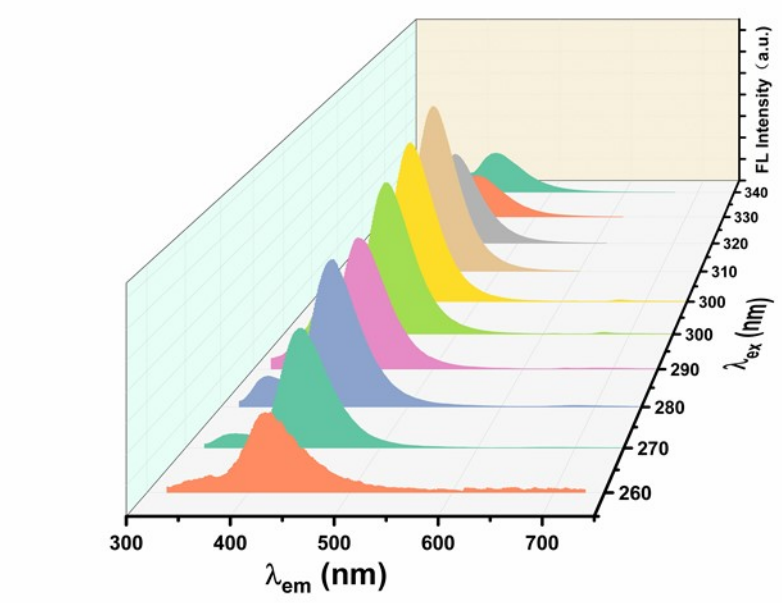

Figure S17. Fluorescence emission of Cu-MOF under the excitation from 260 nm to 340 nm with span of 10 nm.

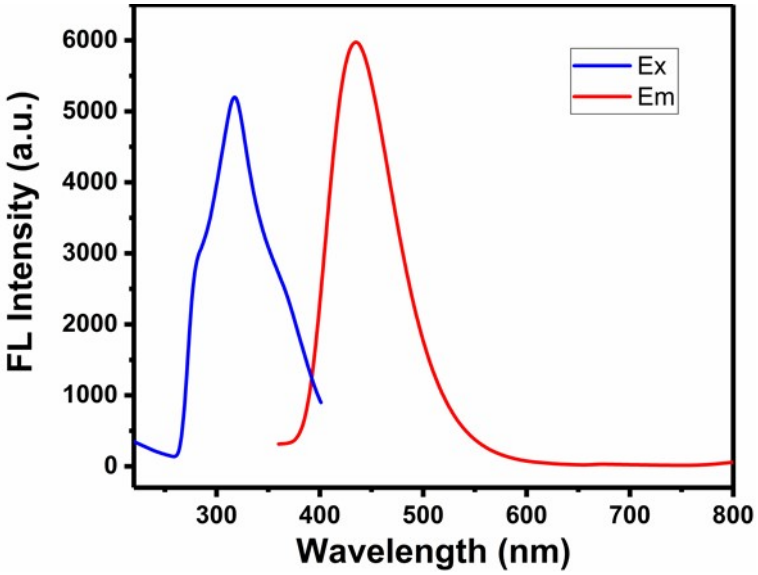

Figure S18. Fluorescence emission and excitation spectra of Cu-MOF in DMF suspensions.

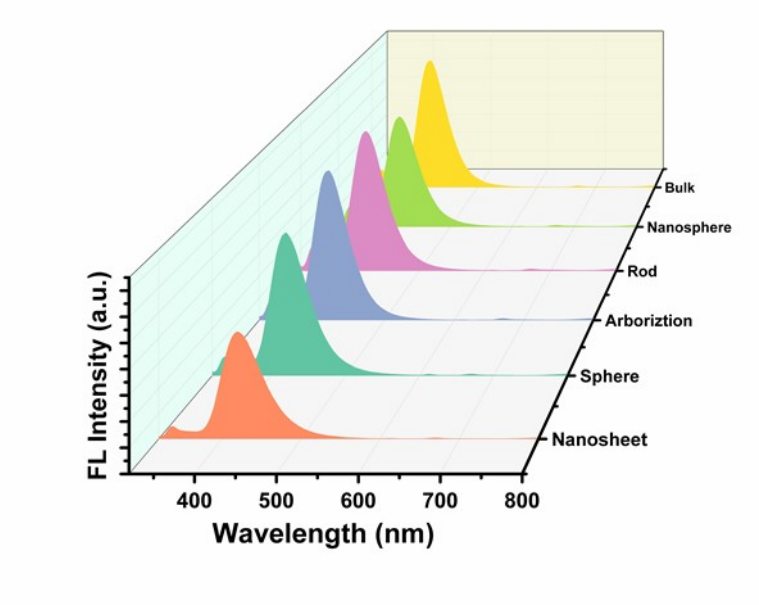

Figure S19. Fluorescence spectra of different morphology Cu-MOF.

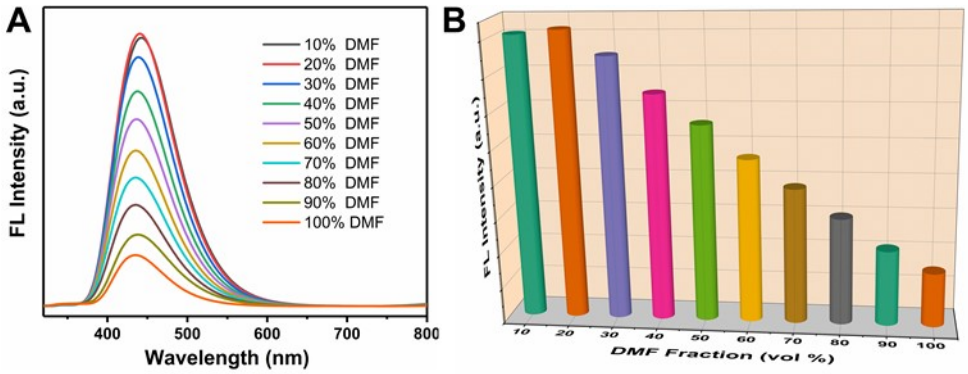

Figure S20. (A) FL spectra of Cu-MOF in DMF/water mixtures with different DMF fraction. (B) The effect of DMF fraction for the Cu-MOF.

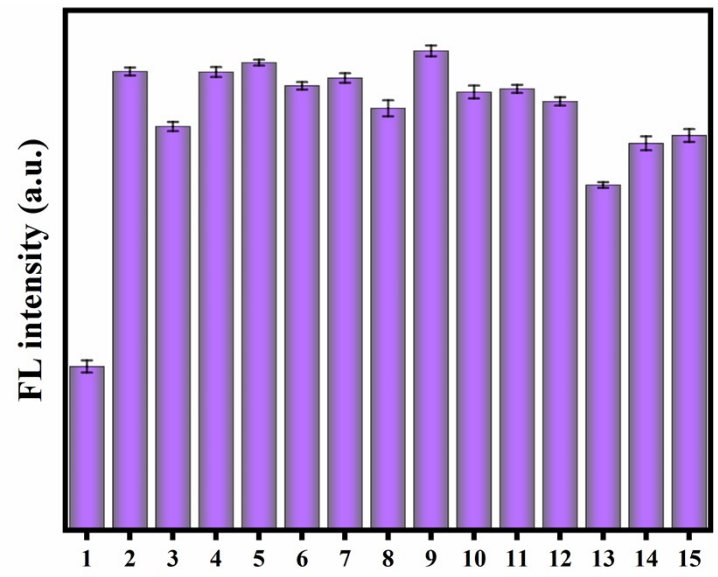

Figure S21. Intensity of Cu-MOF responding to Fe^{3+} with 4-fold other ions. (1) Blank, (2) Fe^{3+}, (3) Fe^{3+}+Ag^{+}, (4) Fe^{3+}+Ca^{+}, (5) Fe^{3+}+SO_4^{2-}, (6) Fe^{3+}+Co^{2+}, (7) Fe^{3+}+Cu^{2+}, (8) Fe^{3+}+Fe^{2+}, (9) Fe^{3+}+CO_3^{2-}, (10) Fe^{3+}+Mn^{2+}, (11) Fe^{3+}+Ni^{2+}, (12) Fe^{3+}+Pb^{2+}, (13) Fe^{3+}+$Cr_2O_7^{2-}$, (14) Fe^{3+}+MnO_7^{2-}, (15) Fe^{3+}+IO_3^{-}

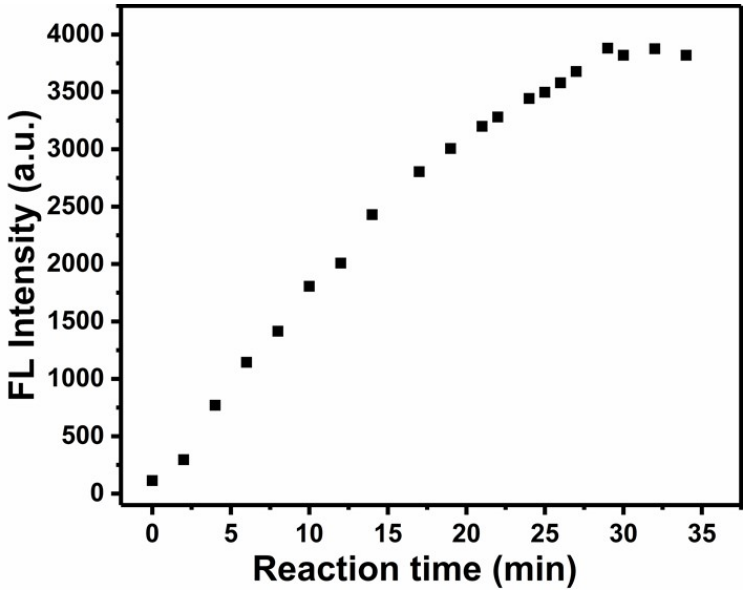

Figure S22. Time-dependent response of Cu-MOF after the addition of Fe^{3+}.

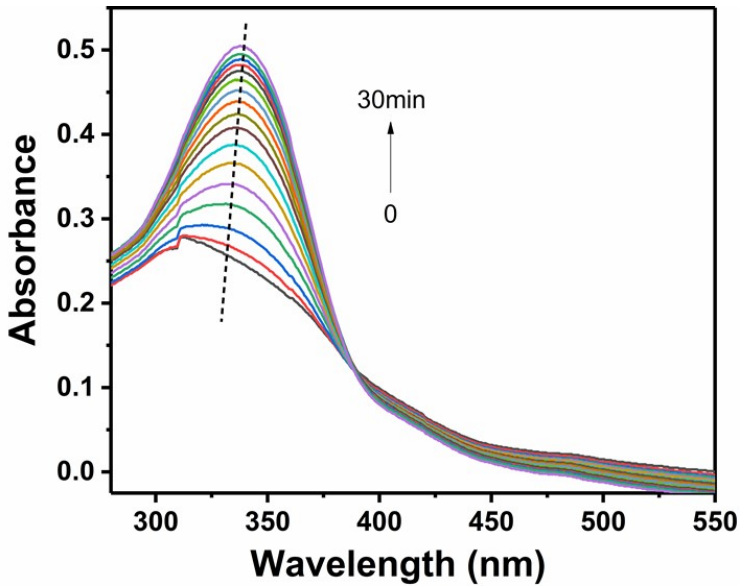

Figure S23. UV-vis spectra of Cu-MOF responding to Fe^{3+} in DMF solution at different times during adsorption from 0 to 30 min.

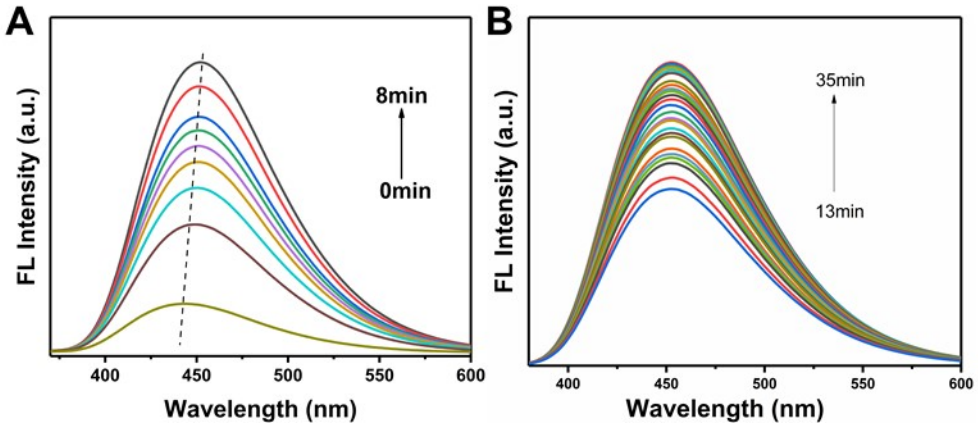

Figure S24. Fluorescence variation of Cu-MOF in DMF with different reaction time: (A)reaction time from 0 to 10 min and (B)reaction time from 13 min to 35 min.

Table S1 The synthetic process of the Cu-MOF with different apparent structure

Samples	DMF	DMA	Ethanol	H_2O	Morphology
A	2		1	1	Bulk
B		1		1	Nanosphere
C		1			Arboriztion
D		2	1	1	Sphere
E	1		1		Rod
F		5		1	Nanosheet

Note: A-F corresponds to Figure 3 (A)-(F).

DMA: N, N'-dimethylacetamide, DMF: N, N'-imethylformamide

Table S2 Results for the detection of Fe and Cu element after Cu-MOF detection by ICP-OES

Element	Testing result (μg/ml)
Fe	0.287
Cu	0.974

Table S3 Results for the detection of Fe^{3+} in real samples.

Targets	Samples	Sample Added (μM)	Measured (μM)	Recovery(%)
Fe^{3+}	Xinkai Lake	0	Not Detected	--
		25	23.6	94.4
		40	38.2	95.5
		65	59.2	91.2

References:

[1] L. Ma, X. Feng, S. Wang, B. Wang, Recent advances in AIEgen-based luminescent metal–organic frameworks and covalent organic frameworks, Materials Chemistry Frontiers, 1 (2017) 2474-2486.

[2] J. Zhang, S. Ren, H. Xia, W. Jia, C. Zhang, AIE-ligand-based luminescent Cd(ii)–organic framework as the first "turn-on" Fe^{3+} sensor in aqueous medium, Journal of Materials Chemistry C, 8 (2020) 1427-1432.

[3] Y. Deng, N. Chen, Q. Li, X. Wu, X. Huang, Z. Lin, Y. Zhao, Highly fluorescent metal–organic frameworks based on a benzene-cored tetraphenylethene derivative with the ability to detect 2, 4, 6-trinitrophenol in water, Crystal Growth & Design, 17 (2017) 3170-3177.

[4] H. Q. Yin, X. Y. Wang, X. B. Yin, Rotation Restricted Emission and Antenna Effect in Single Metal-Organic Frameworks. *J. Am. Chem. Soc.* 141 (2019) 15166– 15173

[5] J. Liu, Y. Ye, X. Sun, B. Liu, G. Li, Z. Liang, Y. Liu, A multifunctional Zr(iv)-based metal–organic framework for highly efficient elimination of Cr(vi) from the aqueous phase, Journal of Materials Chemistry A, 7 (2019) 16833-16841.

[6] R.R.R. Prasad, S.E. Seidner, D.B. Cordes, M.M. Lozinska, D.M. Dawson, M.J. Thompson, T. Düren, K.K. Chakarova, M.Y. Mihaylov, K.I. Hadjiivanov, F. Hoffmann, A.M.Z. Slawin, S.E. Ashbrook, M.L. Clarke, P.A. Wright, STA-27, a porous Lewis acidic scandium MOF with an unexpected topology type prepared with 2,3,5,6-

tetrakis(4-carboxyphenyl)pyrazine, Journal of Materials Chemistry A, 7 (2019) 5685-5701.